Velocity Field Simulation around NACA0012 Airfoil Using SST Turbulence Model at Varied Angles of Attack and Mach Numbers

Jiayao Chen

Department of Agricultural Engineering, College of Engineering, Nanjing Agricultural University, Nanjing Jiangsu 210031, P.R. China

ABSTRACT

Fluid mechanics has gained considerable popularity in current research, owing to its extensive applicability and exceptional performance, which has attracted significant scholarly interest for further investigation and enhancement. This study focuses on the utilization of the SST turbulence model in a two-dimensional framework to conduct simulations of the velocity flow field over the NACA0012 airfoil. The simulations consider varying angles of attack and incoming Mach numbers ①, with the Reynolds number based on the chord length being approximately 6·106. The obtained results reveal a notable correlation between the angle of attack and the degree of streamline twist in the velocity field. Additionally, an increase in the angle of attack leads to a reduction in the high flow velocity region near the leading edge, and the emergence of attached vortices is observed near the suction surface at the trailing edge.

KEYWORDS

Numerical simulation; NACA0012; Velocity flow field; SST turbulence model

DOI: 10.47297/taposatWSP2633-456905.20230402

1 Introduction

With the widespread utilization of fluid machinery, there has been a growing focus on investigating a fundamental constituent - the blade. Of particular significance are the aerodynamic characteristics of blade airfoils, as they exert a substantial influence on the overall efficiency of fluid machinery. Consequently, scholars both domestically and internationally have embarked on numerous investigations and comparisons of diverse airfoil designs in practical applications. Traditional methods for analysis involve water and wind tunnel model experiments, alongside computational fluid dynamics (CFD) numerical simulations and other technical approaches.

However, it is worth noting that water and wind tunnel experiments possess inherent limitations, such as elevated costs and inadequate capacity to capture intricate details [1]. In contrast, the CFD method has emerged as an appealing alternative, offering significant advantages in terms of design cost reduction and airfoil validation time, thus rendering it an ideal means for scrutinizing airfoil performance.

Numerical simulation techniques hold a pivotal role in the analysis of flow fields and are subject to continuous enhancements for various types of fluid machinery investigations. The SST model synergistically incorporates near-wall function and free-flow characteristics, rendering it proficient in accurately simulating diverse internal and external flow phenomena. Given the contemporary prominence of the NACA airfoil, we employ the SST turbulence model to conduct a simulation of the flow field around the NACA 0012 airfoil at a specific angle of attack in this study. Subsequently, the obtained results are subject to comprehensive analysis and examination.

2 Literature Review

In the field of numerical simulation technology, among the prevailing approaches are the separated vortex model, large vortex simulation, super vortex simulation, and Reynolds-averaged turbulence model [2]. While high-precision numerical simulation holds promise for furnishing precise data references and capturing intricate processes, certain challenges remain unaddressed. For instance, the LES method demands impeccable meshes and extensive computational memory, and the S-A model suffers from subpar computational accuracy.

Hu Z [3] et al. used three turbulence models, SST $k-\omega$, LES and DES, to numerically simulate the NACA0009 hydrofoil vane top gap and found that the prediction of DES model was most consistent with the experimental results. Manhart M [4] et al. compared several numerical simulation methods, such as DDES, IDDES, etc., to improve the original model as a basis, but the simulation found that the little success. Kang D [5] et al. used the LES method to numerically simulate the flow field dynamics characteristics of a cleaning robot, and the results showed that the LES method can get effective data to analyse its characteristics. Yang J [6] et al. showed that LES can capture the complete evolution of the separation vortex and provide a theoretical basis for the design of the aircraft.Both DES and LES methods have been gradually used in production practice, but there are some limitations due to the large amount of computation of these two methods.

Gao C [7] et al. used the non-stationary RANS method to carry out high-precision numerical simulation of the vortex wake structure of a coaxial rigid rotor helicopter in hovering state, and found that it can effectively capture the fine structure generating process, and the results show that this method has high computational efficiency and accuracy. Xiao Y [8] et al. used the RANS method, combined with a two-equation turbulence model, to study the open-water performance of a pull-type pod thruster.The RANS method is the most widely used numerical simulation method at present, with a shorter computation time and no high requirements on the quality of the mesh.

3 Design and Method

(1) NACA airfoil design

The symmetric airfoil NACA 0012 airfoil (no curvature, maximum thickness of 0.12 times the chord length) was fitted to the airfoil curves shown in Figure.1, with data from NASA Langley Research Center [9].

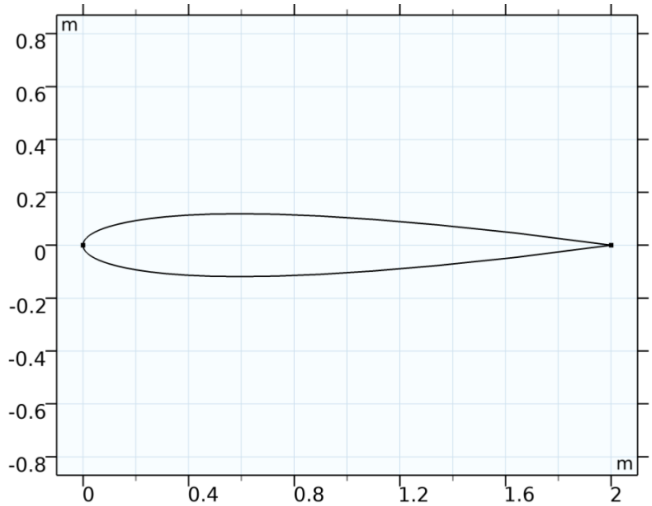

Figure 1. NACA 0012 Airfoils.

The coordinates of its surface (including upper and lower surface points) are calculated as in Equation (1):

$$y = \pm c \cdot 0.594689181 \cdot (0.298222773 \cdot \sqrt{\frac{x}{c}} - 0.127125232 \cdot \frac{x}{c} - 0.357907906 \cdot (\frac{x}{c})^2 + 0.291984971 \cdot (\frac{x}{c})^3 - 0.105174696 \cdot (\frac{x}{c})^4) \tag{1}$$

Apply no-slip conditions on the airfoil surface.

(2) Numerical simulation

In this paper, the reference coordinate system of the NACA 0012 airfoil with a chord length of c = 2.0 m is used as a fixed coordinate system, and the flow field is flowed relative to this coordinate system at an ambient temperature of 20 °C.

Table 1. The figure for free-stream velocity and Mach number.

free-stream velocity (U_∞)	Mach number (M)
34.4 m/s	0.10
51.5 m/s	0.15
68.7 m/s	0.20
85.9 m/s	0.25

The values of the incoming velocity (U_∞) and the incoming Mach number (M) are shown in Table 1.

The data in Table 1 can be obtained from Equation (2) and (3), where C is the speed of sound and T is the temperature:

$$C = 331.6 + 0.6T \tag{2}$$

$$M = \frac{U_\infty}{C} \tag{3}$$

The Reynolds number based on the chord length is about $6 \cdot 10^6$, so the boundary layer can be assumed to be turbulent over the entire airfoil. The angle of inclination (attack angle) of the airfoil with respect to the incoming flow is , and it is easy to see that the relationship with is shown in Equation (4).

$$(u_\infty, v_\infty) = U_\infty(\cos\alpha, \sin\alpha) \quad (4)$$

In order to reduce the possible influence of the boundary conditions on the flow field, the upstream, top and bottom boundaries of the flow domain were set to be located at 100 chord lengths from the trailing edge of the airfoil, and the downstream exit boundary was located at 200 chord lengths from the trailing edge.

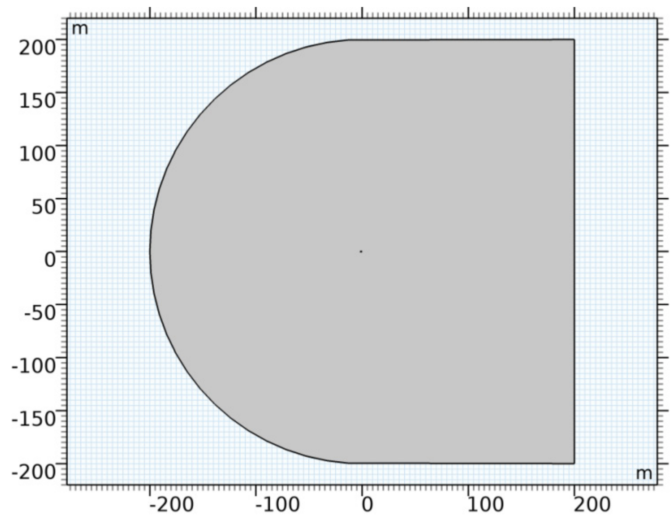

Figure 2. Flow domain.

The values of the turbulence variables for the variables at the far field [10] are calculated according to Equation (5), where the value of the turbulent kinetic energy in the incoming flow is given by Equation(6).

$$\omega_\infty = (1 \to 10)\frac{U_\infty}{L}, \qquad \frac{v_{T\infty}}{v_\infty} = 10^{-(2\to5)} \quad (5)$$

$$k_\infty = v_{T\infty}\omega_\infty \quad (6)$$

L is the length of the front of the computational domain. The turbulence parameters for the incoming flow in the current model use permissive values, obtained from Equation(7).

$$\omega_\infty = 10\frac{U_\infty}{L}, \qquad k_\infty = 0.1\frac{v_\infty U_\infty}{L} \quad (7)$$

The essence of meshing is to split the continuous solution domain by discretization method and then perform discrete computation on multiple regions separately. According to the node distribution law can be divided into structured and unstructured grids. Structured grids have a certain geometric regularity, while unstructured grids do not show a regular distribution [11].

The computational grid in this paper uses a structured grid with a high ratio of dimensions between the outermost cells and the wall-adjacent cells.

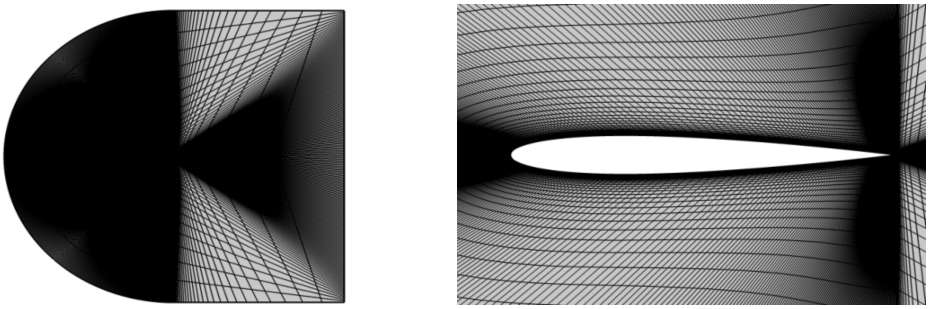

(a) Overall meshing (b) Partial enlargement

Figure 3. Airfoil calculation grid

Two alternatives exist for configuring the initial velocity field: the first entails imposing a constant velocity, while the second involves solving the potential flow equation. The former approach offers simplicity but does not adhere to the no-slip condition required for the setup in this study. In contrast, the latter method provides a more precise and dependable initial approximation. Hence, the current paper adopts the approach of solving the potential flow equation for the setup of the initial velocity field.

Assuming that the flow is spinless and viscous, the velocity potential (φ) is defined as:

$$u = -\nabla\varphi \quad (8)$$

φ must satisfy the continuity equation for incompressible flow in Equation(9):

$$\nabla \cdot u = 0 \quad (9)$$

The continuity equation can be expressed as the Laplace equation as shown in Equation(10):

$$\nabla \cdot (-\nabla\varphi) = 0 \quad (10)$$

This is the potential flow equation.

Once the velocity potential is calculated, the pressure can be approximated using Bernoulli's equation describing steady state flow as shown in Equation(11):

$$p = -\frac{\rho}{2} |\nabla\varphi|^2 \quad (11)$$

In this paper, the flow field at angle of attack $\alpha = 0°, 2°, 4°, 6°, 8°, 10°, 12°, 14°$ are calculated by numerical simulation method.

4 Result

The velocity cloud obtained from the SST turbulence model calculation is shown in Figure.4. At an angle of attack of $0°$, the flow field distribution has roughly the same trend at different incoming Mach numbers. The flow lines are uniformly distributed with the symmetry axis of the straight line where the centre axis of the airfoil is located, but obvious low velocity zones appear near the leading and trailing edges. The flow velocity is higher near the upper and lower airfoils of the airfoil, and it is worth noting that the extent of the high velocity zone increases with the increase of the incoming flow Mach number.

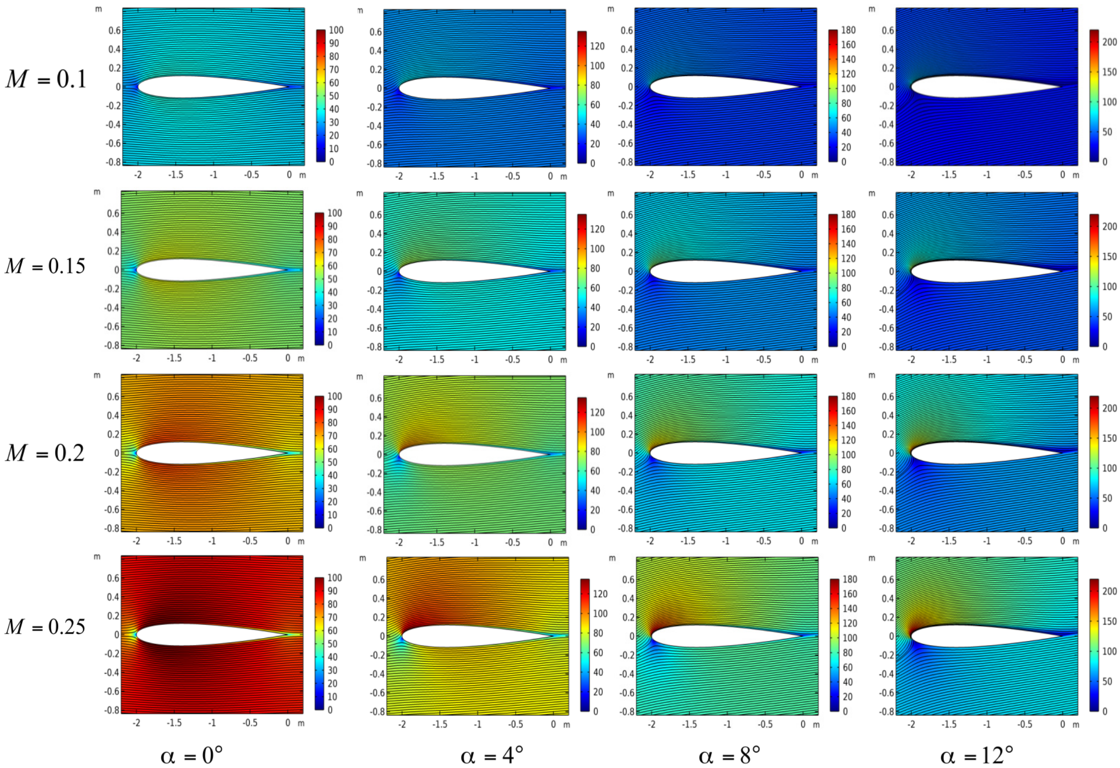

Figure 4. Velocity field cloud map

When the angle of attack is not $0°$, the velocities of the upper and lower airfoils of the airfoil behave differently, with the velocity of the upper airfoil near the leading edge region being significantly higher than that of the lower airfoil. This tendency is especially obvious when the angle of attack is $4°$ and $8°$. When the angle of attack is $4°$, the high flow velocity area ranges from about 0 to 0.5c on the upper airfoil, and the maximum velocity occurs near the leading edge, and then gradually decreases, and basically returns to the same velocity as that on the lower airfoil at the trailing edge. The leading and trailing edge streamlines were twisted to different degrees. As the Mach number of the incoming flow increases, the range of the high flow velocity area increases. When the angle of attack is $8°$, the high flow velocity area ranges from 0 to 0.3c on the upper airfoil, and the leading and trailing edge streamlines are twisted to a greater extent, but the other trends are the same as when the angle of attack is $4°$. When the angle of attack is $12°$, the high flow velocity zone ranges from about 0 to 0.2c on the upper airfoil, and the leading and trailing edge streamlines are twisted most violently.

5 Conclusion

Drawing from the velocity cloud map results, the following conclusions are ascertained:

(1)An increase in the angle of attack leads to a heightened degree of streamline twisting within the velocity field. Notably, the streamlines adjacent to the leading edge exhibit a pronounced counterclockwise twist with a larger rotation angle, whereas the phenomenon of streamline twisting near the trailing edge remains less conspicuous. Intriguingly, variations in the incoming Mach number at a given angle of attack do not exert any influence on the degree of streamline twisting.

(2) At a constant incoming Mach number, elevating the angle of attack results in a reduction of the high-flow velocity region near the leading edge, while inducing the appearance of attached vortices near the suction surface at the trailing edge. However, it is noteworthy that the overall velocity in the velocity field remains unaffected by these changes.

About the Author

Jiayao Chen is undergraduate of Nanjing Agricultural University, and her research field is Engineering.

Notes

① Mach number, in fluid mechanics, is the ratio of the velocity of a fluid to the velocity of sound in that fluid.

References

[1] Xie K, Laith K.Abbas, Chen D, et al. (2019). Numerical simulations on dynamic stall of a complex motion of airfoil under unsteady freestream velocity. Journal of Harbin Engineering University, 40(05):865-71.

[2] Wang F. (2016). Research progress of computational model for rotating turbulent flow in fluid machinery. Transactions of the Chinese Society for Agricultural Machinery, 47(02):1-14.

[3] Hu Z, Yang F, Wang X, et al. (2022) .Feasibility analysis of detached eddy simulation in tip leakage flow simulation. Large Electric Machine and Hydraulic Turbine, 284(05):59-67.

[4] Manhart M, Friedrich R. (2002) .DNS of a turbulent boundary layer with separation. International Journal of Heat & Fluid Flow, 23(5):572-81.

[5] Kang D, Xiong T, et al. (2023). Large eddy simulation on flow field of cleaning robot under oblique flow. Ship Engineering, 45(04):21-26+158.

[6] Yang J, Gao J, et al. (2023). A study on flow separation of NACA0012 airfoil based on LES. Journal of Civil Aviation Flight School of China, 34(02):10-14.

[7] Gao C, Song W, et al. (2023). High-accurate numerical simulation of wake vortex over coaxial rigid rotor helicopter in hover. Flight Dynamics, 41(02):14-20.

[8] Xiao Y, Mao Y, et al. (2021) .On scale effect of open water performance of puller podded propulsors based on RANS. Journal of Ship Mechanics, 25(12):1606-22.

[9] NASA Langley Research Center, Turbulence Modeling Resource. (2022). 2D NACA 0012 airfoil validation case. http://turbmodels.larc.nasa.gov/naca0012_val.html

[10] Menter, F.R. (1994). Two-equation eddy-viscosity turbulence models for engineering applications. AIAA Journal, 32, 1598-1605.

[11] Kim H J, Lee S, Fujisawa N. (2006) .Computation of unsteady flow and aerodynamic noise of NACA0018 airfoil using large-eddy simulation. International Journal of Heat & Fluid Flow, 27(2):229-42.